Eur. Phys. J. B 43, 3–9 (2005)
DOI: 10.1140/epjb/e2005-00021-y

THE EUROPEAN PHYSICAL JOURNAL B

Optoelectronic properties of zinc blende ZnSSe and ZnBeTe alloys

S. Abdi-Ben Nasrallah, S. Ben Afia, H. Belmabrouk[a], and M. Said

Unité de Recherche de Physique des Solides, Département de Physique, Faculté des Sciences de Monastir, 5019 Monastir, Tunisia

Received 15 May 2004 / Received in final form 15 August 2004
Published online 11 February 2005 – © EDP Sciences, Società Italiana di Fisica, Springer-Verlag 2005

Abstract. The compositional dependence of the electronic band structure has been computed for zinc blende ZnS_xSe_{1-x} and $Zn_{1-x}Be_xTe$ alloys with composition x ranging from 0 to 1. The empirical pseudo potential method with the virtual crystal approximation have been used. A particlar attention has been paid to the effect of alloy disorder on the electronic properties of the II-VI studied compounds. For this purpose, the compositional disorder is added to the virtual crystal approximation as an effective potential. Such correction approximates significantly our calculated values of the band gap bowing parameters to experimental ones. The ZnS_xSe_{1-x} gap energy shows a nonlinear behavior with strong bowing for low compositions of sulfur. The $Zn_{1-x}Be_xTe$ compound, as it is known, can be direct or indirect semiconductor depending on its beryllium composition x. The electron effective mass and the refractive index have been investigated as well. Polynomial approximations are obtained for both the energy gap and the effective mass as functions of alloy composition at Γ and X valleys.

PACS. 71.20.Nr Semiconductor compounds – 71.15.-m Methods of electronic structure calculations – 71.15.Dx Computational methodology (Brillouin zone sampling, iterative diagonalization, pseudopotential construction)

1 Introduction

Due to their scientific and technological interest, the semiconductor (SC) compounds IV, III-V and II-VI have been extensively studied. The quality of II-VI materials has been lower than that of Si and III-V ones due to croissance problems, high band polarity and doping limits. However, in spectral region where Si and III-V (SC) cannot provide the required band gap, the II-VI with the nitrides are the best candidates to cover a large range of the visible spectrum. In last years, with progress in crystal growth technology, researches on wide bandgap II-VI (SC) has been undertaken. Nevertheless, this is particularly due to important specifities namely great excitonic effects and magnetic aspect which lead to spin electronic. The study of excitons allows the local detection of free and trapped carriers and the important oscillator strength leads to a splitting more important than that obtained with GaAs or GaInAs. Furthermore, the introduction of a magnetic ion (Mn or Mg) introduces a ferromagnetic interaction between localised spins and free carriers.

Experimental and theoretical studies on wide bandgap semiconductors such as ZnSe, ZnS, BeTe, ZnTe and their heterostructures have been undertaken [1]. This interest is motivated by the possibility to control the band gap energy and the lattice constant at the design of new light emitters or detectors operating in specific spectral range (blue region for ZnSe [2] and UV for ZnS). Mixed crystal AB_xC_{1-x} attracts more and more interest as disorder model systems [3,4]. By changing the alloy composition, physical properties can be controlled at any value between those of the binaries AC and AB [5]. This offers the possibility to adapt the material in devices by choosing the alloy with the appropriate lattice constant which matched to a number of substrates. ZnS_xSe_{1-x} is a good candidate as an optoelectronic material. With a direct gap ranging from 2.80 eV (ZnSe) to 3.67 eV (ZnS), it spans an interesting region for light emitters. It is also used as waveguides and confinement layers in laser diodes (LDs). For example, ZnS_xSe_{1-x} with x composition larger than 0.2 is used as a cladding layer [6]. However, if a blue LD is needed, $ZnS_{0.06}Se_{0.94}$ ($x = 0.06$) lattice matched to GaAs is used as an active layer [7].

The beryllium compounds are potentially good materials for technological applications [8,9]. However, they are difficult to handle experimentally presumably because of their toxic nature. Furthermore, only a few of theoretical results are available [10,11]. Tellurures have shown remarkable results on microcavities, diluted magnetic semiconductors and hybrid structures. Diodes based on ZnTe are favoured on their concurrent GaN. Indeed, ZnTe green emission is more pure than blue-green radiation of GaN

[a] e-mail: Hafedh.Belmabrouk@fsm.rnu.tn

Table 1. Pseudopotential form factors and lattice constants for zinc-blende ZnSe, ZnS, ZnTe and BeTe.

compound	V^{S} (3) (Ryd)	V^{S} (8) (Ryd)	V^{S} (11) (Ryd)	V^{A} (3) (Ryd)	V^{A} (4) (Ryd)	V^{A} (11) (Ryd)	lattice constant (nm)
ZnSe	−0.383536	0.021660	0.094511	−0.140184	0.062	−0.035802	0.56686 [16]
ZnS	−0.226152	0.03	0.061513	0.223987	0.14	0.04	0.54093 [16]
ZnTe	−0.227428	0.0	0.07581	0.0386	0.05	−0.0075	0.61037 [17]
BeTe	−0.428823	−0.021065	0.254048	−0.221772	0.120	0.259592	0.56250 [18]

and its fabrication is easier. $\mathrm{Zn}_{1-x}\mathrm{Be}_x\mathrm{Te}$ alloy is a promising material as another choice for p-contact layer since it can be lattice matched to a number of commercially available substrates as GaAs, InP and ZnSe by adjusting the alloy composition. In particular, $\mathrm{Zn}_{1-x}\mathrm{Be}_x\mathrm{Te}$ alloys with $x = 0.08$ and 0.05 are lattice matched with ZnSe and GaAs respectively [9]. The ZnBeTe alloy has the advantage to contain only one group VI element II-II-VI. Therefore, the composition control is easier in comparison with II-VI-VI ternaries. Cho et al. [9] found that the ZnBeTe films have good composition controllability and can be highly p-type doped ($p > 10^{19}$ cm^{-3}) using active nitrogen plasma. Interface properties between the ZnBeTe/GaAs will be much better than either ZnSe/GaAs or ZnSSe/GaAs because the tellurium has lower reactivity with GaAs surface than sulfur or selenium [12]. In spite of the importance of these ternaries, their electron properties are not sufficiently investigated and need additional studies at least from the theoretical point of view.

To this aim, we report in this paper calculation of electron band parameters of common anion (ZnBeTe) and common cation (ZnSSe) compounds. In Section 2, we present the computational method namely the empirical pseudo potential method within the virtual crystal approximation (VCA). The results related to band gap energy, electron effective masses and refractive index are reported and discussed in Section 3.

2 Computational method

To compute the electronic band structure of binary compounds, the empirical pseudopotential method (EPM) has been used [13]. In order to obtain the atomic form factors $V(G)$, where G is a reciprocal lattice vector, a non linear least square method is used. This fitting procedure consists on the minimization of the difference between the calculated band gaps at the high-symmetry points and the experimental ones. For the zinc blende structure, only six pseudopotential form factors are considered [14,15]. To achieve convergence, 136 plane waves are taken into account. The obtained form factors and lattice constants for zinc blende ZnSe, ZnS, ZnTe and BeTe are listed in Table 1.

It is straightforward to extend our treatment to ternary alloys $\mathrm{AB}_x\mathrm{C}_{1-x}$ through the use of the virtual crystal approximation (VCA) [19,20]. The symmetric and antisymmetric form factors for alloys of interest can be expressed as a function of those of the binary parents

$$V_{\mathrm{ABC}}^{\mathrm{S,A}}(G) = (1-x)\,V_{\mathrm{AC}}^{\mathrm{S,A}} + x\,V_{\mathrm{AB}}^{\mathrm{S,A}}. \qquad (1)$$

The alloy constant lattice is obtained according to Vegard's rule:

$$a_{\mathrm{AB}_x\mathrm{C}_{1-x}} = (1-x)a_{\mathrm{AC}} + x a_{\mathrm{AB}}. \qquad (2)$$

Using this lattice constant, the corresponding reciprocal lattice vectors and the pseudopotential form factors $V^{\mathrm{S,A}}(G)$ of equation (1), we can calculate the band structures of alloys.

It is well known that the VCA does not take into account the effect of compositional disorder [21] and hence the bowing factors obtained by VCA may deviate from experiments. In order to overcome this shortcoming, we have added to the VCA a non-periodic potential due to the compositional disorder [22]. This method will be called the 'improved VCA'. By adding this effective disorder potential, the expression (1) becomes:

$$V_{\mathrm{ABC}}^{\mathrm{S,A}} = (1-x)V_{\mathrm{AC}}^{\mathrm{S,A}} + xV_{\mathrm{AB}}^{\mathrm{S,A}} - p\sqrt{x\,(1-x)}\,\left[V_{\mathrm{AC}}^{\mathrm{S,A}} - V_{\mathrm{AB}}^{\mathrm{S,A}}\right]. \qquad (3)$$

p is then treated as an adjustable parameter.

The refractive index is also an important optical property. Actually, the use of fast non-destructive optical techniques for epitaxial layer characterisation is limited by the accuracy with which refractive indices can be related to alloy composition. Many attempts have been made to correlate energy band gap to refractive index of semiconductors. Moss [23] proposed the following relation:

$$E_g n^4 = 95 \text{ eV}. \qquad (4)$$

Ravindra and Srivastava [24] proposed a value of 108 eV instead of 95 eV. But this relation based on an atomic model is limited. Gupta and Ravindra [25] suggested a linear relation given by:

$$n = \alpha + \beta\, E_g \qquad (5)$$

with $\alpha = 4.084$ and $\beta = -0.62$ eV^{-1}.

Herve and Vandamme [26] proposed a relation based on the classical oscillator theory and given by:

$$n = \sqrt{1 + \left(\frac{\alpha}{E_g + \beta}\right)^2} \qquad (6)$$

Table 2. Band-gap energies of ZnSe, ZnS, ZnTe and BeTe at Γ, X and L points.

Material	E_g^{Γ} (eV)	E_g^{X} (eV)	E_g^{L} (eV)
ZnSe	**2.80**; 2.80 [7,13,27]	**4.49**; 4.49 [13]	**3.92**; 3.92 [13]
ZnS	**3.67**; 3.67 [13]	**5.23**; 5.23 [13]	**5.22**; 5.22 [13]
ZnTe	**2.27**; 2.27 [8,28]	**3.05**; 3.05 [29]	**2.68**; 2.38 [17]
BeTe	**4.1**; 4.1 [8,29]	**2.8**; 2.8 [8,29]	**3.57**; 3.57 [30]

where $\alpha = 13.6$ eV and $\beta = 3.4$ eV.

The high frequency dielectric constant (ε_∞) is calculated using the relation $\varepsilon_\infty = n^2$.

We note that Moss relation uses only one parameter for all materials, while the relations (5) and (6) use a set of two parameters. On the other hand, Herve and Vandamme formula is derived for a wide range of materials while Gupta and Ravindra relation is more specific for semiconductors and approximates the experimental gaps in the range of energy band gap from 0.5 to 3.5 eV [25].

3 Results and discussion

Band gap energies for ZnSe, ZnS, ZnTe and BeTe in zinc blende structure have been calculated. The values of these gaps at the high symmetry points are listed in Table 2. For all binary compounds our calculated energy gaps E_g^{Γ}, E_g^{X} and E_g^{L} (in bold numbers) agree well with experimental data. This shows that the calculated form factors are satisfactory.

3.1 Band gap energy of ZnS_xSe_{1-x}

The band gap energies E_g^{Γ}, E_g^{X} and E_g^{L} of ZnS_xSe_{1-x} are calculated within VCA ($p = 0$). In Figure 1, the results are plotted versus the sulfur composition x in the alloy (solid line). Two different behaviors are clearly observed. The curves exhibit a pronounced minimum and an important bowing for small compositions whereas they have a little deviation from linear behavior and a small bowing for the remaining range of x. Similar behaviors were observed in ZnSeTe [31], ZnSTe [32], ZnCdS [33], ZnCdSe [34], ZnCdTe [35] , CdSSe [36], BeCdSe [37] II-VI alloys. We attempt to fit our results, in the first step, according to the common used expression:

$$E_g(x) = (1-x)\,E_g(\text{ZnSe}) + x\,E_g(\text{ZnS}) - b\,x\,(1-x)$$

where b is the so-called bowing parameter that is assumed to be constant. The two-degree polynomial fit versus x does not agree satisfactory with the calculated energy band gaps $E_g^{\Gamma}(x)$ and $E_g^{L}(x)$. This leads us to use a higher polynomial degree. The best fits obtained are:

$$E_g^{\Gamma}(x) = 2.78 - 2.10\,x + 7.54\,x^2 - 4.57\,x^3$$
$$E_g^{X}(x) = 4.42 - 3.00\,x + 3.92x^2$$
$$E_g^{L}(x) = 3.93 - 3.78\,x + 10.17\,x^2 - 5.09\,x^3.$$

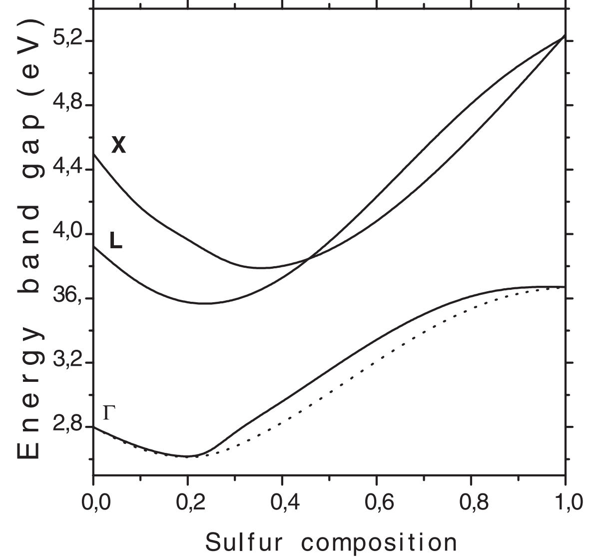

Fig. 1. The band gaps versus the sulfur composition at Γ, X and L points in zinc- blende ZnS_xSe_{1-x} calculated without compositional disorder (solid line) and at Γ point calculated with compositional disorder (dashed lines).

For E_g^{Γ} and E_g^{L}, it appears clearly that the bowing parameter b depends on the sulfur composition. To approximate our bowing parameter b to the experimental one available in literature for $x = 0.5$ ($b = 0.63$ eV) [38], E_g^{Γ} has been calculated using the improved VCA. The best concordance is obtained for $p = 0.05$. Figure 1 (dashed lines) presents the energy E_g^{Γ} versus the sulfur composition x with compositional disorder. The best fit of E_g^{Γ} is when the compositional disorder is taken into account:

$$E_g^{\Gamma}(x) = 2.80 - 2.26\,x + 7.55\,x^2 - 4.43\,x^3.$$

This result shows clearly that b depends strongly on the sulfur composition x:

$$b(x) = -4.43\,x + 1.13.$$

Figure 1 indicates that the curve is altered by the presence of compositional disorder but it has the same appearance. The band gap shows firstly a decreasing trend as x increases, then an increase with a linear behavior. For x around 1, we have a saturation tendency. The decrease of energy band gap bowing is extremely important for laser applications or lattice matched quantum wells. As expected, the maximum effect of disorder is observed

Table 3. Calculated high-frequency dielectric constants (ε_∞) for ZnS_xSe_{1-x} alloy using EPM within improved VCA and available experimental data.

Material	High frequency dielectric constant (ε_∞)			
	Moss relation	Gupta and Ravindra relation	Herve and Vandamme relation	Experiment: reference [39]
ZnSe	5.82	5.51	5.80	5.4
$ZnS_{0.3}Se_{0.7}$	5.92	5.78	5.96	
$ZnS_{0.5}Se_{0.5}$	5.56	4.75	5.42	
$ZnS_{0.7}Se_{0.3}$	5.25	3.80	4.95	
ZnS	5.08	3.25	4.69	5.1

for $x = 0.5$. This behavior of the band gap in the small range of x can be explained as follows: for small values of x, the sulfur composition is yet small and cannot disturb the ZnSe. Thus, the energy gap decrease is not due to the compositional disorder but it can be attributed to the electronic interactions. Indeed, the differences in electro negativity and in ionic or covalent radius of sulfur and selenium entrain differences between band lengths and angles, so additional interactions appear.

The calculated band gap energy can be used to estimate the refractive index for the alloys using the above mentioned models. The calculated values of the high frequency dielectric constant $\varepsilon_\infty = n^2$ are listed in Table 3 for some values of sulfur composition. Experimental data are available only for binaries ZnSe ($\varepsilon_\infty = 5.4$) and ZnS ($\varepsilon_\infty = 5.1$). In view of this table, we can notice that the Gupta and Ravindra expression gives better results with respect to the experiment as compared to Moss and Herve and Vandamme relations for ZnSe which has a band gap lesser than 3.5 eV. However, for ZnS with a band gap equal to 3.8 eV, the agreement between our results and the experimental data is not as good as for ZnSe. The Moss relation approximates better experiments for high band gaps.

3.2 Electron effective mass of ZnS_xSe_{1-x}

Due to the importance of electron effective mass m_e^* in the discussion of transport properties and exciton effects in semiconductors, we present in this paragraph, our calculated values at the conduction band minima. We determine m_e^* from the band structure by adopting a parabolic relation of $E(k)$ versus the wave vector k.

The variation of the electron effective mass at Γ and X points versus the sulfur composition for ZnS_xSe_{1-x} with and without disorder is displayed in Figure 2; it is evaluated in units of the free electron mass m_o. As can be seen, the disorder influences weakly the electron effective mass at Γ point but it has no effect at X point. Therefore, the effect of the compositional disorder proves to depend on wave vector k so on energy. At Γ point (plot a), a nonlinear variation is obtained according to the following expression:

$$m_e^*(x) = 0.186 + 0.019\,x + 0.087\,x^2 \quad \text{(without disorder)}$$
$$m_e^*(x) = 0.193 - 0.064\,x + 0.160\,x^2 \quad \text{(with disorder).}$$

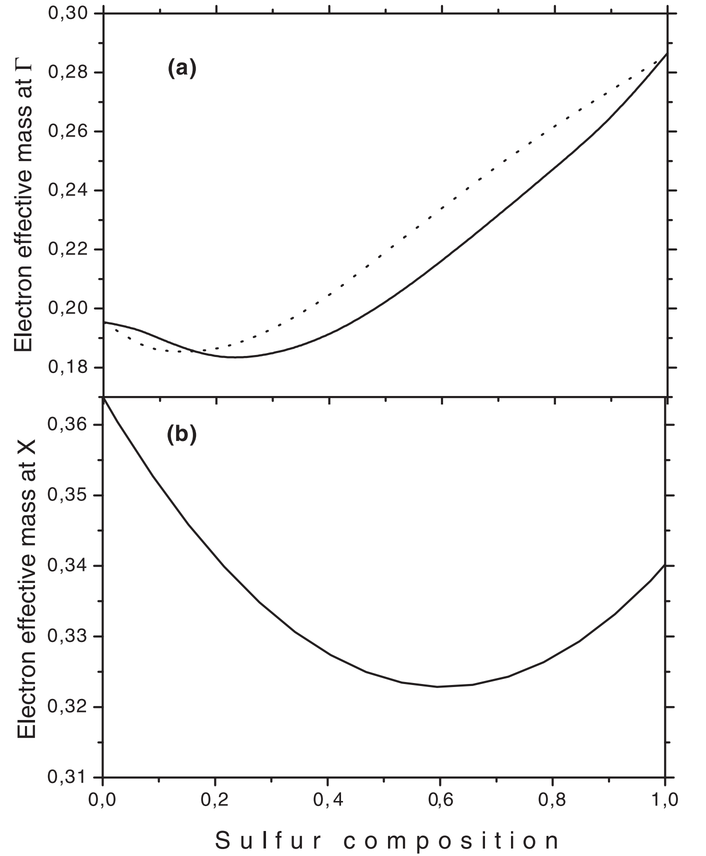

Fig. 2. The electron effective mass of Γ (plot a) and X (plot b) valleys in cubic ZnS_xSe_{1-x} as a function of sulfur composition x. The solid and dashed lines correspond to calculations without and with disorder respectively.

The calculated value of m_e^* for cubic ZnSe ($m_e^* = 0.19$ in m_o) agrees reasonably well with the experimental data, $m_e^* = 0.21$ and $m_e^* = 0.17$ given respectively in references [40,41]. However, it is higher than that obtained by k.p method, $m_e^* = 0.16$ reference [16]. For ZnS compound, a good agreement is obtained between our calculated value ($m_e^* = 0.28$) and that of 0.28 and 0.27 reported respectively in references [42,43].

At X point (plot b), the best fit of electron effective mass variation versus the sulfur composition has the form:

$$m_e^*(x) = 0.36 - 0.14\,x + 0.11\,x^2.$$

Table 4. Calculated high-frequency dielectric constants (ε_∞) for $Zn_{1-x}Be_xTe$ alloy using EPM within improved VCA and available experimental data.

Material	High frequency dielectric constant (ε_∞)			
	Moss relation	Gupta and Ravindra relation	Herve and Vandamme relation	Experiment reference [45]
ZnTe	6.46	7.15	6.74	7.30
$Zn_{0.7}Be_{0.3}Te$	5.80	5.45	5.77	
$Zn_{0.5}Be_{0.5}Te$	5.85	5.60	5.85	
$Zn_{0.3}Be_{0.7}Te$	2.43	2.40	2.43	
BeTe	4.81	2.37	4.28	

In particular, $m_e^* = 0.36$ for ZnSe and 0.33 for ZnS. Unfortunately, the lack of experimental and theoretical results in literature at X point prevents us to approve our calculated values.

3.3 Band gap energy of $Zn_{1-x}Be_xTe$

The second alloy studied ZnBeTe is a common anion compound. The electronic properties such as band gap and electron effective mass have been investigated. Figure 3 shows the variation of E_g^Γ and E_g^X versus the beryllium composition x without disorder (solid line). The $E_g^\Gamma(x)$ and $E_g^X(x)$ curves can be fitted by the equations:

$$E_g^\Gamma(x) = 2.26(1-x) + 4.12x$$
$$E_g^X(x) = 3.04(1-x) + 2.79x + 1.66x(1-x).$$

Maksimov et al. [29] reported for $x = 0.5$ the bowing parameter of $b = 0.5$ eV. To reproduce better the experimental results we are lead to use a disorder parameter p depending on the beryllium composition x. The direct Γ-Γ and indirect Γ-X band gaps versus x are shown in Figure 3 (dashed lines) and fitted by:

$$E_g^\Gamma(x) = 2.26\,(1-x) + 4.13\,x$$
$$E_g^X(x) = 3.04\,(1-x) + 2.801x - 0.67\,x\,(1-x).$$

The direct gap exhibits a linear dependence on the whole range of x. It increases linearly with beryllium at a rate of 18.6 meV for change of 1% in beryllium. This is in good agreement with [10,29]. For the Γ-X indirect band gap, the bowing parameter 0.67 eV is near of reference [10]. The direct to indirect crossover occurs at $x \approx 0.30$. This value reproduces satisfactory result of reference [44] which reports a value of $x \approx 0.28$. So we can distinguish two regions: one direct band gap Γ-Γ for $0 \le x \le 0.3$ and another indirect band gap Γ-X for $0.3 \le x \le 1$. It should be noted, that the disorder does not influence E_g^Γ curve. But it has an important effect on E_g^X. This means that the disorder effect depends not only on the beryllium composition x but also on the energy.

Using the calculated $E_g(x)$ and according to the relations 4–6, we have calculated the refractive index of $Zn_{1-x}Be_xTe$ as a function of x and then deduced the high frequency dielectric constant $\varepsilon_\infty = n^2$. Our results are summarized in Table 4. The use of Gupta and Ravindra gives for ZnTe $\varepsilon_\infty = 7.18$ which is in good agreement with experimental value $\varepsilon_\infty = 7.30$ of reference [45]. However, the beryllium chalcogenures are recent alloys and there is no experimental or theoretical data reported to BeTe.

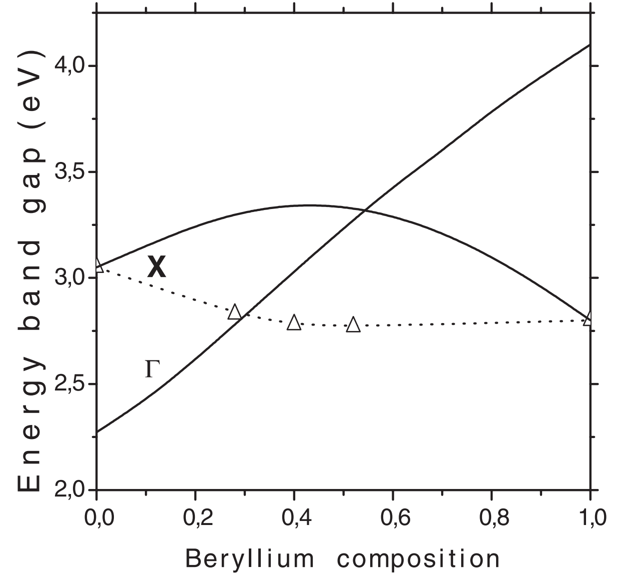

Fig. 3. The band gaps versus beryllium composition x at Γ and X points in zinc-blende $Zn_{1-x}Be_xTe$ calculated without compositional disorder (solid line) and with compositional disorder (dashed lines). Also we reported experimental results at X [29] (triangles).

3.4 Electron effective mass of $Zn_{1-x}Be_xTe$

The electron effective mass m_e^* for the ternary $Zn_{1-x}Be_xTe$ is calculated as a function of beryllium composition x. For the direct gap region, $0 \le x \le 0.3$, results are displayed in Figure 4. Our obtained value of electron effective mass for ZnTe ($m_e^* = 0.20$ in m_o) is in good agreement with experimental data of reference [40] ($m_e^* = 0.2$). However, it is greater than that obtained by k.p method ($m_e^* = 0.12$) [41]. In the range of compositions $0.3 \le x \le 1$, the band gap is indirect (Γ-X), the band conduction is some what flat and does not show

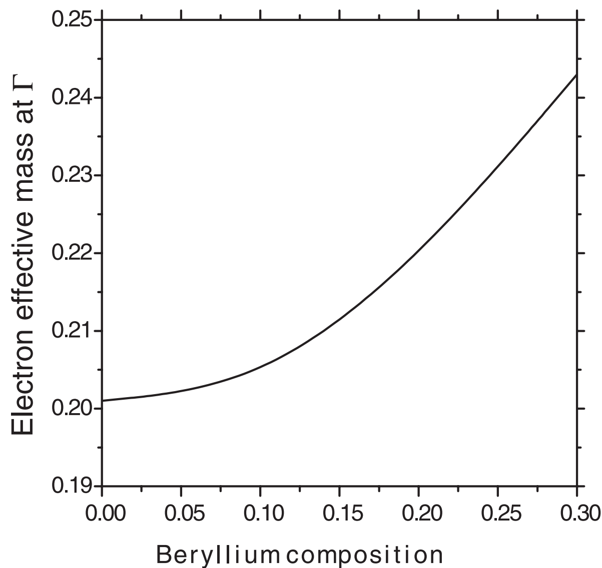

Fig. 4. The electron effective mass of Γ valley in $Zn_{1-x}Be_xTe$ versus the beryllium composition x.

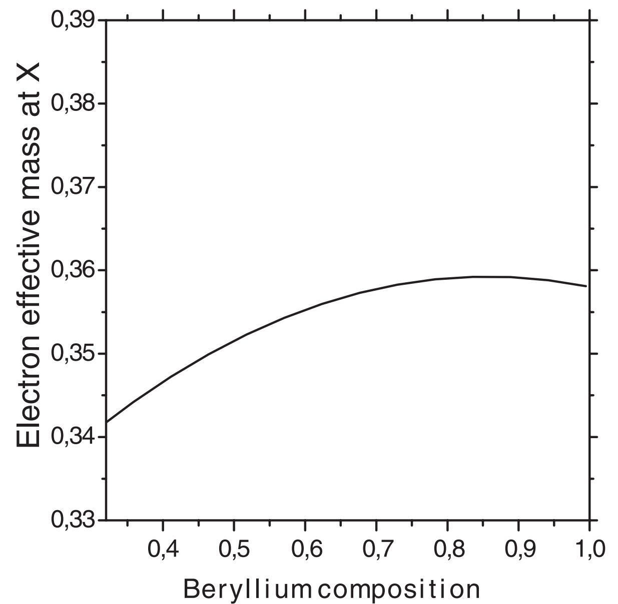

Fig. 5. The electron effective mass of X valley in $Zn_{1-x}Be_xTe$ versus the beryllium composition x.

a clear minimum so the effective mass does not show a significant change versus x. The difference between the extremum values is 6%. For BeTe, the calculated value of electron effective mass is 0.35. Unfortunately in our knowledge, there is no report of experimental or theoretical data for BeTe.

4 Conclusion

We have used the EPM under the VCA to calculate the electron properties of ZnS_xSe_{1-x} and $Zn_{1-x}Be_xTe$ in zinc blende phase. The compositional disorder is taken into account by adding a non periodic potential to the VCA. The band gap energy, the electron effective mass as well as the refractive index has been computed versus the alloy composition.

In the aim to obtain a good agreement with experimental gaps in the high symmetry points, we are lead to use a disorder parameter depending on alloy composition and energy. For the ZnSSe alloy, the bowing depends on the sulfur composition and the band gap energy exhibits a decrease for small molar fractions. Presumably, unexpected behaviour arises from either chemical disparity or difference in lattice constants. As a result, the atoms shift from initial symmetry positions, giving an additional deformation potential. Such a potential is at the origin of the deviation of the electron band parameters from a linear trend.

This study provides useful information to simulate heterostructures in the II-VI system for designing optoelectronic devices aimed to operate in the blue wave length range. The ZnBeTe ternary which has an indirect band gap region from x higher than 0.3 eV is useful for devices in microelectonics.

References

1. P. Rodriguez-Hernandez, M. Gonzalez-Diaz, A. Munoz, Appl. Sur. Sci. **124**, 445 (1998)
2. A. Waag, F. Fisher, H.J. Lugauer, Th. Litz, J. Laubender, U. Lunz, U. Zehnder, W. Ossau, T. Gerhardt, M. Moller, G. Landwer, J. Appl. Phys. **80**, 792 (1996)
3. M. Quillec, *Materials for Optoelectronics* (Kluwer Academic Publishers, Boston, 1996)
4. R.N. Dupuis, J.C. Camphell, J.R. Velebir, J. Crystal Growth **75**, 598 (1986)
5. N. Bouarissa, R. Bachiri, Z. Charifi, Phys. Status Solidi (b) **226**, 293 (2001)
6. N. Teraguchi, S. Hirata, H. Mouri, Y. Tomomura, A. Suzuki, H. Takiguchi, J. Crystal Growth **150**, 803 (1995)
7. H. Okuyama, K. Nakano, T. Miyajima, K. Akimoto, J. Crystal Growth **117**, 139 (1992)
8. S.-B. Che, I. Nomura, W. Shinozaki, A. Kikuchi, K. Shimomura, K. Kishino, J. Crystal Growth **214**, 321 (2000)
9. M.W. Cho, S.K. Hong, J.H. Chang, S. Saeki, M. Nakajima, T. Yao, J. Crystal Growth **214/215**, 487 (2000)
10. A. Munoz, P. Rodriguez, A. Mujica, Phys. Status Solidi (b) **198**, 439 (1996)
11. P.E. Van Camp, V.E. Van Doren, Solid State Commun. **98**, 741 (1996)
12. A. Oktaz, L.H. Kuo, T. Yasuda, K. Kimara, S. Miwa, T. Yao, K. Nakejima, K. Kimura, J. Vac. Sci. Technol. B **15**, 1254 (1997)
13. M.L. Cohen, J.R. Chelikowsky, *Electronic Structure and Optical Properties of Semiconductors* (Springer, Berlin, 1988)
14. P.Y. Yu, M. Cardona, *Fundamentals of Semiconductors*, 1st edn. (Springer, 1996)
15. M.L. Cohen, T.K. Bergstresser, Phys. Rev. **141**, 789 (1966)

16. H. Mayer, U. Rossler, Solid State Communications **87**, 1417 (1993)
17. G.-D. Lee, M.H. Lee, J. Ihm, Phys. Rev. B **52**, 1459 (1995)
18. D. Gerthsen, T. Walter, F. Fisher, T. Gerhand, A. Waag, G. Landwher, J. Crystal Growth **214/215**, 330 (2000)
19. L. Bellaiche, S.-H. Wei, A. Zunger, Appl. Phys. Lett. **70**, 3558 (1997)
20. L. Bellaiche, D. Vanderbilt, Phys. Rev. B **61**, 7877 (2000)
21. A. Zunger, S. Mahajan, *Handbook on Semiconductors*, Vol. 3 (Elsevier, New York, 1994)
22. S-H. Wei, L.G. Ferreira, J.E. Bernard, A. Zunger, Phys. Rev. B. **42**, 9622 (1990)
23. T.S. Moss, Phys. Status Solidi (b) **131**, 415 (1985)
24. N.M. Ravindra, V.K. Srivastava, Infrared Phys. **19**, 603 (1979)
25. V.P. Gupta, N.M. Ravindra, Phys. Status Solidi (b) **100**, 715 (1980)
26. P.J.L. Herve, L.K.J. Vandamme, Infrared Phys. Thechnol. **35**, 609 (1994)
27. K. Wilmers, T. Wethkamp, N. Esser, C. Cobet, W. Richter, M. Cardona, V. Wagner, H. Lugauer, F. Fischer, T. Gerhard, M. Keim, Phys. Rev. B **59**, 10071 (1999)
28. M.Th. Litz, K. Watanabe, M. Korn, H. Ress, U. Lunz, W. Ossau, A. Waag, G. Landwehr, Th. Walter, B. Neubauer, D. Gerthsen, U. Schüssler, J. Crystal Growth **159**, 54 (1996)
29. O. Maksimov, M.C. Tamargo, Appl. Phys. Lett. **79**, 782 (2001)
30. M.-G. Diaz, P.-R. Hernandez, A. Munoz, Phys. Rev. B **55**, 14043 (1997)
31. F.C. Peiris, S. Lee, U. Bindley, J.K. Furdyna, J. Appl. Phys. **86**, 719 (1999)
32. R. Hill, D. Richardson, J. Phys. C **6**, L115 (1973)
33. L.G. Suslina, A.G. Plyukhin, D.L. Fedorov, I.-A. Nauk, Ser. Fiz. **40**, 1194 (1976)
34. A.G. Areshkim, G. Spkar, G.N. Polisskii, T.B. Popova, L.G. Suslina, D.L. Fedorov, Fiz. Tverd. Tela. **28**, 3743 (1986)
35. D.J. Olego, J. Faurie, S. Sivan, P. Mraccak, Appl. Phys. Lett. **47**, 1172 (1985)
36. O. Goede, D. Henning, L. John, Phys. Status Solidi (b) (6) **96**, 671 (1979)
37. S.V. Ivanov, O.V. Nekrutkina, S.V. Sorokin, V.A. Kaygorodov, T.V. Shubina, A.A. Toropov, P.S. Kop'ev, G. Reuscher, V. Wagner, J. Geurts, A. Waag, G. Landwehr, Appl. Phys. Lett. **78**, 404 (2001)
38. L. Soonckindt, D. Etienne, M. de Murcia, G. Bougnot, Thin. Solid. Films **70**, 285 (1980)
39. O. Madelung, *Semiconductors Basic Data*, 2nd revised edn. (Springer, 1996)
40. D.W. Palmer, *The Semiconductors-Information, Properties of the II-VI compound semiconductors, 2002*
41. K. Shahzad, D.J. Olego, C.G. Van de Walle, Phys. Rev. B **38**, 81 (1987)
42. J.C. Miklosz, R.G. Wheeler, Phys. Rev. B **153**, 913 (1967)
43. S.J. Czyzak. W.M. Baker, R.C. Gane, J.B. Have, J. Opt. Soc. Am. **3**, 240 (1975); T.M. Biemewski, S.J. Czyzak, J. Opt. Soc. Am. **53**, 496 (1963)
44. M.R. Buckley, F.C. Peiris, O. Maksimov, M. Munoz, M.C. Tamargo, Appl. Phys. Lett. **81**, 5156 (2002)
45. W.A. Harrison, *Electronic Structure and the Properties of Solids* (Dover Publications, INC, New York, 1989)